DOI: 10.1002/ejic.201001239

Covalent Functionalization of Silicon Surfaces with a Cavitand-Modified Salen

Cristina Tudisco,[a] Giuseppe Trusso Sfrazzetto,[a] Andrea Pappalardo,[a] Alessandro Motta,[a] Gaetano A. Tomaselli,[a] Ignazio L. Fragalà,[a] Francesco P. Ballistreri,[a] and Guglielmo G. Condorelli*[a]

Keywords: Silicon / Surface chemistry / Monolayers / Metalation / Cavitands

Si(100) and porous silicon substrates have been engineered with cavitand modified salen molecules. A salen derivative, specifically designed for covalently anchoring on silicon, was grafted onto Si(100) surfaces by photochemical hydrosilylation, and onto porous silicon by thermal hydrosilylation. These hybrid systems have been studied by different analytic techniques. Monochromatized X-ray photoelectron spectroscopy (XPS) was used to characterize both flat and porous samples. Atomic force microscopy (AFM) and, in particular, atomic force lithography (AFL) were used to evaluate the monolayer structure and morphology of the flat silicon surface, while Fourier transform infrared spectroscopy (FTIR) was adopted to probe the hydrosilylation process involving porous samples. The uranyl complex of the salen derivative was directly synthesized on the silicon surface by the reaction between Si-anchored salen and uranyl acetate. This surface-based synthesis suggests that the salen molecules are intact and keep their specific properties after silicon anchoring.

Introduction

The use of organic molecules to impart specific surface properties has been a subject of intense research not only from a fundamental research perspective, but also because of the many technological applications these systems are suitable for.[1] In this context, the functionalization of inorganic surfaces with organic monolayers[2] is an attractive approach to develop hybrid materials, with tuned functional properties, that are suitable for a variety of applications.[3] Several workers have explored the use of molecular monolayers as active layers in thin-film interfaces,[4] molecular devices,[5] molecular magnets[6] and various sensors.[7] In this last field, considerable contributions that have assisted in the development of new receptors have been given by synthetic organic chemistry, and many systems have been synthesized with molecular recognition properties based on specific interactions and shape complementarity.[8] Nevertheless, any synthetic effort remains useless for most practical applications unless the organic receptors are assembled in solid devices. For such applications, monolayer-based sensors have several advantages compared to both thin films and bulk materials for which the weak signals due to the interactions between surface layers and analytes are often covered by the signals due to the bulk layers. Given the ubiquitous use of silicon in microelectronic devices, the covalent anchoring of synthetic receptors on Si represents a key aim in the development of Si-integrated sensing materials, and some examples of supramolecular receptors grafted on monocrystalline Si(100) have been recently reported.[9–11]

This paper reports on the synthesis and the covalent anchoring onto silicon of a quinoxalinic cavitand modified with *N*,*N*′-bis(salicylaldehyde) ethylenediimine (salen), receptor **1**, which has been functionalized with an undecylenic group for Si anchoring (Scheme 1). The processes of covalent anchoring of this cavitand onto both monocrystalline Si(100) and porous silicon (**PSi**) have been investigated since both of these substrates are of technological interest. Si(100) is, in fact, the surface of choice for the development of commercial microelectronic devices, whilst porous silicon represents an interesting candidate for novel devices due to its specific properties such as high surface area and luminescence.[12]

1-functionalized monocrystalline silicon (**Si-1**) and porous silicon (**PSi-1**) were characterized by XPS, which is an ideal tool for obtaining molecular information relating to nanometric layers. AFM and, in particular, AFL were used to evaluate the structure and morphology of the functionalized Si(100) surface, while FTIR was adopted to probe the grafting of **1** onto **PSi**.

The functionality of the hybrid **Si-1** surface was tested by reacting **Si-1** with uranyl acetate solution. In this way a salen uranyl complex was obtained directly on the **Si-1** surface via a 2D surface synthetic route.[2a] It is well known that chiral uranyl-salen complexes act as receptors for enan-

[a] Dipartimento di Scienze Chimiche, University of Catania and INSTM Udr of Catania,
V.le A. Doria 6, 95125 Catania, Italy
Fax: +39-095-580-138
E-mail: guido.condorelli@unict.it

Supporting information for this article is available on the WWW under http://dx.doi.org/10.1002/ejic.201001239.

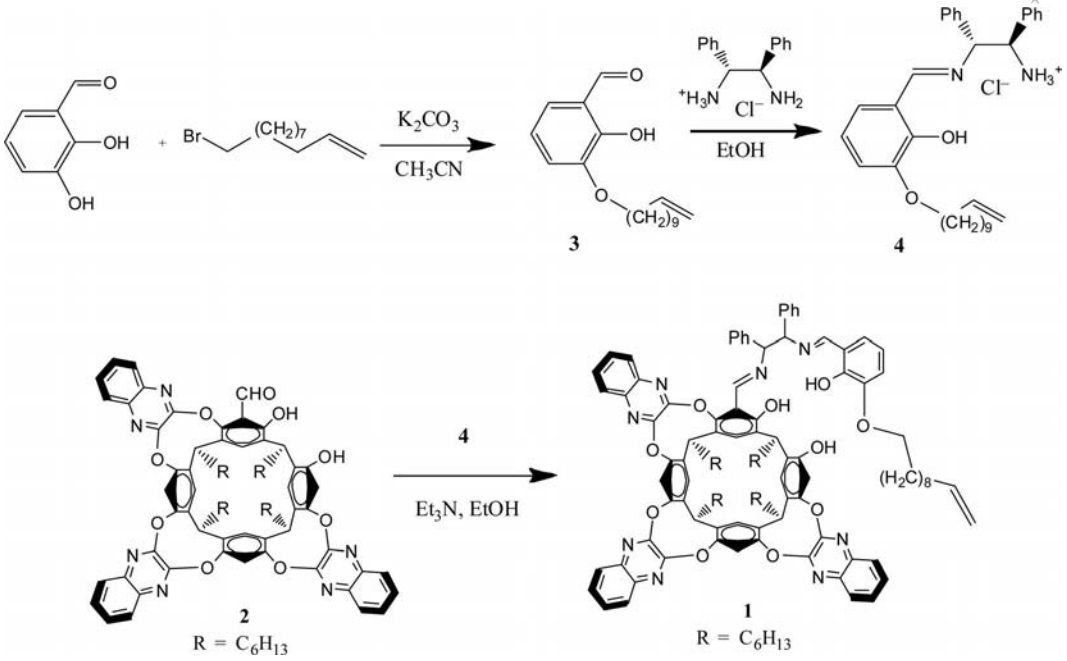

Scheme 1. Procedure for the synthesis of the salen derivative **1**.

tioselective molecular recognition, due to the fact that they are able to recognize anions by exploiting the Lewis acidity of the uranyl centre that equatorially coordinates with anions.[13d–13e] The uranyl-salen complex derived from receptor **1** behaves as a heteroditopic receptor in which the metal centre is able to coordinate the anion, whereas the π-rich quinoxalinic cavity binds tetraalkylammonium cations by stabilizing them with CH···π and cation···π interactions. The synthesis of the uranyl-salen complex on **Si-1** was performed with a double purpose: (i) to evaluate possible surface routes towards metal-salen complexes, and (ii) to prove that after silicon anchoring the salen molecules are intact and keep their specific molecular properties. To validate the complexation results, control experiments on native silicon oxide and alkyl-functionalized surfaces were also performed.

Results and Discussion

*Cavitand-salen **1**. Synthesis and complexation properties:* A cavitand-modified salen suited for silicon anchoring (**1**) was synthesized (according to Scheme 1) from the monoformyl cavitand **2**.[13,14] The reaction of 3-hydroxysalicylaldehyde with 11-bromo-1-undecene leads to compound **3**. Condensation of **3** with (1*R*,2*R*)-(+)-diphenylethylenediamine chloride[13a] affords the monoimine ammonium chloride derivative **4**. Monoformyl cavitand **2** was finally converted into the enantiopure receptor **1** by treatment with compound **4** in the presence of triethylamine. Compounds **1**–**4** were fully characterized by NMR and EI-MS techniques. Salen **1** is a receptor that possesses two different binding sites. The first site is a quinoxalinic cavity that is active for tetraalkylammonium ions binding,[15] and the complexation properties of which have been determined from solution experiments (see Supporting Information). The second site is a salen-derived moiety based on a bis(salicylidene)-1,2-diphenylethylenediimine group that is active for the complexation of metallic cations such as Mn^{III} and UO_2^{VI}.[13]

*XPS characterization of **Si-1** and **PSi-1**:* Cavitand-salen **1** was grafted onto H-terminated Si(100) surfaces via photochemical hydrosilylation of the double bonds, while thermal-driven hydrosilylation was adopted for grafting of **1** onto **PSi**.

The **1**-functionalised monocrystalline and porous silicon-based materials (**Si-1** and **PSi-1**) were characterized by XPS. Table 1 compares the elemental compositions of two reference samples, namely HF-etched silicon (a) and HF-etched **PSi** (b), with freshly prepared **Si-1** (c), aged **Si-1** (d) and freshly prepared **PSi-1** (e).

Table 1. XPS determined atomic concentrations for (a) HF-etched Si; (b) HF-etched **PSi**; (c) fresh **Si-1** (d) aged **Si-1** and (e) **PSi-1**.

	Atomic concentration			
	Si 2p	O 1s	C 1s	N 1s
(a) HF-etched Si	77.0	7.8	15.2	–
(b) HF-etched **PSi**[a]	76.7	7.6	15.7	–
(c) Fresh **Si-1**	58.5	17.8	23.0	0.7
(d) Aged **Si-1**	47.6	29.7	22.0	0.7
(e) **PSi-1**[a]	28.4	22.0	47.7	1.8

[a] A small amount of residual Ag (Ag < 0.2%) was found in the **PSi** substrates.

The XPS data show that C 1s signals are observed for both reference samples due to the ubiquitous and adventitious presence of contaminant species.[16] However, both the **Si-1** and **PSi-1** surfaces show a significant enhancement of C 1s related signals compared to both the HF-etched Si and **PSi** samples. This enhancement, and especially the

presence of N 1s signals due to the quinoxaline and salen moieties, is an indication of the grafting of **1** onto the substrate surfaces. From XPS data (Table 1), the surface density of salen **1** on monocrystalline Si(100) has been estimated[17] to be ca. 6×10^{12} molecules/cm^2, this leads to a molecular footprint of 16 nm^2 for each molecular unit. This footprint size is much higher than the density functional theory (DFT) estimated cross-sectional area of **1** (ca. 4 nm^2), and therefore this experimentally determined size indicates a low surface coverage.

Useful information on the nature of the grafted layers was obtained from high resolution spectra of the relevant photoemission bands.

The Si 2p spectra of the freshly etched Si and **PSi** surfaces show bands due to a doublet (at 99.2 and 99.8 eV, respectively) associated with elemental silicon (Si^0). After grafting **1** onto the surfaces, the Si 2p spectra of both **Si-1** and **PSi-1** show, besides the Si^0 $2p_{3/2\text{-}1/2}$ doublet, broad bands at 103.0 eV[17] that are consistent with the presence of oxidized silicon in the samples (Figure 1). The intensity of this band in the spectrum of thermal grafted **PSi** is slightly higher than the intensity of the same band in the spectrum of UV grafted **Si-1**, but after aging (1 week) the oxidation levels of the two samples became comparable.

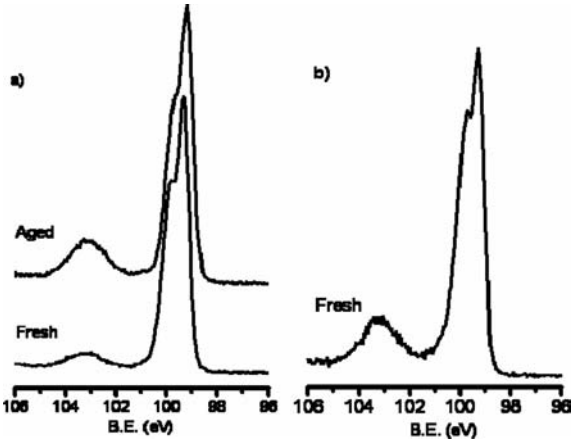

Figure 1. High resolution Si 2p XPS spectra of (a) fresh **Si-1** and 1 week aged **Si-1**, and (b) fresh **PSi-1**. The Si 2p spectrum of **PSi** does not change after aging.

The presence of surface oxidation indicates that the monolayers are not densely packed, which is in accordance with the low surface coverage estimated from the XPS data in Table 1. This result is not unexpected since the larger size of the cavitand moiety compared to the alkyl foot precludes a close packing arrangement. The high resolution C 1s spectra (Figure 2) of **Si-1** and **PSi-1** are similar, and consist of three main peaks: (i) a component at 285.0 eV (C^0) due to the aliphatic and aromatic hydrocarbon backbone of **1** and "adventitious" carbon; (ii) a component at 286.3 eV (C^{+1}) due to oxidized carbon bonded to one oxygen atom (or double bonded to nitrogen) in the cavitand phenyl rings,[9] salen moiety,[18] as well as in the Si–O–C frameworks of "adventitious" contaminants,[6,9,19] and (iii) a third component at 287.7 eV due to the quinoxalinic carbons that bond to oxygen and nitrogen atoms.[9] The broad band detectable in the spectrum of **PSi-1** at approximately 291.5 eV can be assigned to the π-π* shake-up of aromatic rings.[20] The same band in the **Si-1** spectrum cannot be discerned from the background due to the much lower absolute amount of **1** on the flat surface of Si compared to number of molecules of **1** on the porous surface of **PSi**. No relevant change in the C 1s band shape occurs after aging of the samples.

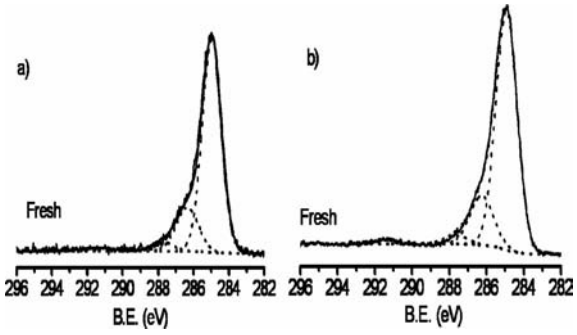

Figure 2. High resolution C 1s XPS spectra of (a) fresh **Si-1** and (b) fresh **PSi-1**. C 1s spectra of **Si-1** and **PSi-1** do not change after sample aging.

High resolution data for the N1s region of the XPS spectra of fresh and aged **Si-1** samples and of **PSi-1** samples are shown in Figure 3. The signals in the N 1s spectral regions give a clear indication of the surface anchoring of **1** in these samples.

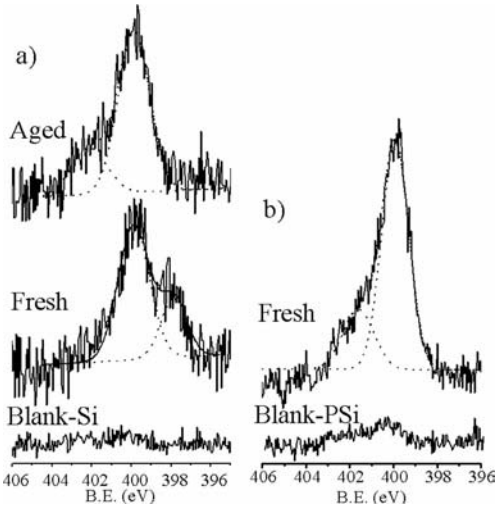

Figure 3. (a) High resolution N 1s XPS spectra of aged **Si-1** (upper), fresh **Si-1** (middle) and **blank-Si** (bottom); (b) High resolution N 1s XPS spectra of fresh **PSi-1** (upper) and **blank-PSi** (bottom). The N 1s spectrum of **PSi-1** does not change after sample aging.

The N1s band in the spectrum of freshly prepared **Si-1** consists of two components: (i) a main component at 399.8 eV (N_{qx}) that is assigned to the quinoxaline nitrogen atoms,[9,18] and (ii) a less intense component at 398.0 eV (N_{sal}) that is assigned to the iminic nitrogen atoms[21] of the salen. The observed intensity ratio N_{qx}/N_{sal} is about 3, which is as expected from the molecular structure. After

one week of sample aging, the N 1s band shape changes (Figure 3) even though the total amount of nitrogen remains constant (Table 1). The N 1s spectrum of the aged **Si-1** samples consists of the same main components; the N_{qx} band is at 399.8 eV whilst the N_{sal} component (denoted as N_{salH}) is shifted to a higher binding energy (N_{salH} at 401.7 eV) than the signal in the spectrum of the freshly prepared sample. This energy shift can be explained either by the formation of hydrogen bonds or by the protonation[22] of the salen nitrogen atoms due to the presence of acidic O_xSi–OH groups on the oxidized surface ($pK_a \approx 4.5$).[23] Moreover, the N_{qx}/N_{salH} intensity ratio is about 3, which is consistent with the atomic ratio between the quinoxalinic and salen nitrogen atoms.

The N 1s band in the high resolution XPS spectrum of **PSi-1** is similar to that observed in the spectrum of aged **Si-1**. It consists of a N_{qx} component at 399.8 eV and a component at 401.8 eV that is due to protonated or H-bonded salen nitrogen atoms (N_{salH}). The intensity ratio N_{qx}/N_{salH} is equal to 3, which is equivalent to the ratio observed in the spectrum of aged **Si-1**. Note that the surface oxidation (Figure 1), and hence the availability of acidic O_xSi–OH groups on **PSi-1**, is comparable to the aged **Si-1** surface; this explains why there are similar interactions (H-bonding or protonation) involving the salen nitrogen atoms in **PSi-1** as in aged **Si-1** samples.

To rule out any possible physisorption and to demonstrate the covalent anchoring of **1** on both flat and porous silicon, **blank-Si** and **blank-PSi** samples have been obtained by processing the Si and **PSi** surfaces with the same treatment adopted for **Si-1** and **PSi-1**, but in the absence of UV irradiation and heating, respectively. The N 1s regions in the XPS spectra of these samples are reported in Figure 3. The spectra do not show any significant signal in the N 1s region, which indicates the absence of physisorbed **1** in these samples. This result provides proof that the grafting of **1** onto the Si and **PSi** surfaces occurs only under either UV irradiation or heating (200 °C), processes which promote the hydrosilylation of the olefin groups and the formation of Si–C bonds.

*FTIR characterization of **PSi-1**:* FTIR measurements provided useful information for monitoring the grafting reaction of **1** onto **PSi** substrates by taking advantage of the high surface area of the porous samples. FTIR spectra of HF-etched **PSi**, **blank-PSi** and **PSi-1** samples are compared in Figure 4. In particular, three spectral regions are reported: (a) the C–H stretching region between 3200 and 2600 cm^{-1}, (b) the Si–H stretching region between 2300 and 1900 cm^{-1} and (c) the region between 1300 and 600 cm^{-1} in which SiO_x stretching vibrations and some bending modes are present. The presence in the **PSi-1** spectrum (Figure 4, a) of intense bands due to the CH_2 symmetric [$\nu_s(CH_2)$] and antisymmetric [$\nu_a(CH_2)$] stretches at 2858 cm^{-1} and 2926 cm^{-1}, respectively, and of a shoulder at 2956 cm^{-1} due to the CH_3 antisymmetric stretch [$\nu_a(CH_3)$], combined with the absence of the homologous stretches in the spectrum of HF-etched **PSi** and with the negligible intensity of these signals in the **blank-PSi** spectrum, is consistent with the thermal anchoring of **1** onto the **PSi** surface. These results are supported by the evolution of Si–H features in the spectra as the grafting reaction progresses. The spectrum of HF-etched **PSi** (Figure 4, b) shows intense bands at 2087 cm^{-1}, 2106 cm^{-1} and 2142 cm^{-1} due to SiH, SiH_2 and SiH_3 stretches of H-terminated **PSi**, respectively.[24] After grafting **1** onto the **PSi** surface, the intensities of the SiH_x bands clearly decrease (Figure 4, b, **PSi-1**) due to the hydrosilylation reaction between Si–H terminations and the double bonds of **1**. Note that a new broad feature appears at 2260 cm^{-1} due to oxygen back-bonded SiH groups (mainly O_3SiH),[24] which are formed because of silicon oxidation. On the other hand, the **blank-Si** spectrum shows an intense band due to SiH_x stretches (2150–2080 cm^{-1}), indicating that no hydrosilylation reaction occurred with this sample. In addition, two new features are observed (Figure 4, b, **blank-Si**) at 2260 cm^{-1} and 2200 cm^{-1}, which can be assigned to Si–H stretches of the O_3SiH and O_2SiH species of the oxidized surface, respectively.[24,25]

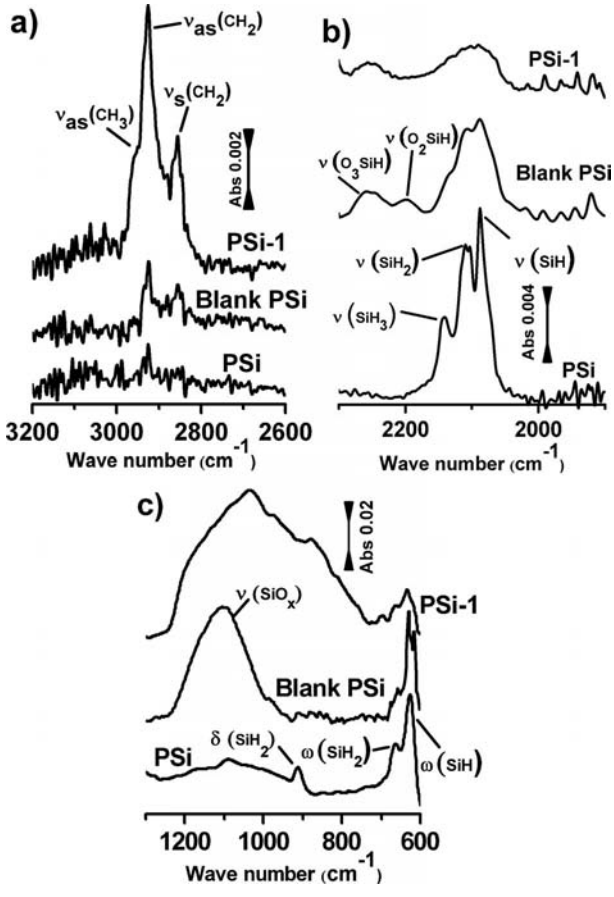

Figure 4. FTIR spectral regions between (a) 3200–2600 cm^{-1} (C–H stretching region), (b) 2300–1900 cm^{-1} (Si–H stretching region) and (c) 1300–600 cm^{-1} (SiO_x stetching and bending modes) of HF-etched **PSi**, **blank-PSi** and **PSi-1**. The transmission spectrum of Si(100) has been subtracted from these spectra as the background.

The 1300–600 cm^{-1} region of the FTIR spectrum of HF-etched **PSi** (Figure 4, c) shows two intense bands at 660 cm^{-1} and 625 cm^{-1} that are due to the wagging vibration modes of SiH_2 and SiH, respectively, and the spec-

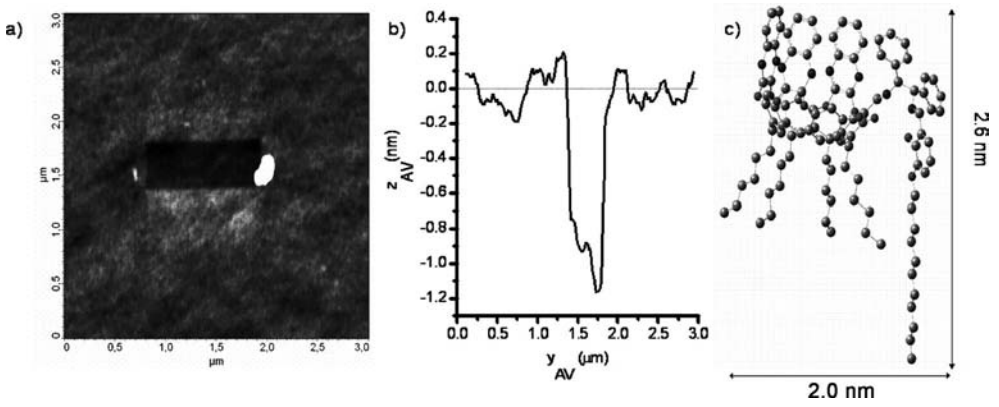

Figure 5. (a) AFM image of **Si-1** after AFL, (b) average cross-section profile of **Si-1** surface scratch and (c) DFT estimated height of **1**. The large feature on the scratch edge is due to the material removed from the scratch.

trum also shows the SiH_2 bending vibrations (δSiH_2) at 910 cm^{-1}.[24c] In the **PSi-1** spectrum, the intensity of these features strongly decrease, analogously to the Si–H stretching signals, due to the hydrosilylation reaction. The 1300–600 region of the **PSi-1** FTIR spectrum is dominated by a broad band centred at 1040 cm^{-1} that is assigned to the vibrational modes of SiO_2.[26] In the spectrum of the **blank-PSi** sample, Si–H wagging modes are intense even though silicon oxide vibrations centred at 1110 cm^{-1} are also present.[25]

*AFM lithography on **Si-1:*** AFM studies were carried out on HF-etched Si and flat **Si-1** samples. AFM topographic images of **Si-1** show a uniform surface with measured statistical parameters (mean height R_{mean} = 1.1 nm and roughness *RMS* = 0.21 nm) that are slightly higher than measured for HF-etched Si (R_{mean} = 0.3 nm and *RMS* = 0.11 nm). Since AFM images do not have enough resolution to discern single molecules, AFL (contact mode)[27] has been used to evaluate the structure of the functionalized surface.[28] Thus, grafted molecules of **1** were removed by rastering different surface areas ($0.5 \times 1.5\ \mu m^2$) with the AFM tip under a suitable constant force (0.24 μN). The thus obtained scratches have an average depth of 1.1 ± 0.2 nm (Figure 5). Such a value is lower than that expected for **1** with an extended configuration. DFT geometry optimization was performed on **1** with a linear configuration and gave a molecular length of 2.6 nm (Figure 5, c). These differences can be explained by either assuming a folded configuration for the molecules. or by considering a model, previously proposed, of a low density monolayer with silicon oxidation of the surface.[28] It has been observed that in these systems, SiO_x islands (with thicknesses of around 1 nm) can intercalate organic molecules.[28] Since the SiO_x islands that grow between the salen molecules cannot be scratched during ALF due to their greater hardness compared to organic molecules,[28] the overall scratch depth results obtained in these measurements are lower than the estimated length of **1**.

Surface synthesis of uranyl complexes: **Si-1** surface reactions have been performed to test 2D surface routes for the preparation of metal-salen complexes and to demonstrate that salen maintains its molecular functionalities after grafting onto the Si surface. Reactivity towards uranyl ions has been evaluated for different functionalized surfaces, the active **Si-1** and, as control experiments, native silicon oxide **SiO_x/Si** and decyl-functionalized Si (**Si-decyl**), by treating samples with ethanol solutions of uranyl acetate. Figure 6 compares high resolution U 4f regions of the XPS spectra of **Si-1** and the reference samples (**SiO_x/Si** and **Si-decyl**) after uranyl treatment. Peaks associated with U 4f7/2 and U 4f5/2 at 382.1 eV and 392.7 eV, respectively, are evident in the spectrum of uranyl treated **Si-1**, which indicates the presence of U^{VI} species in this sample.[29,30]

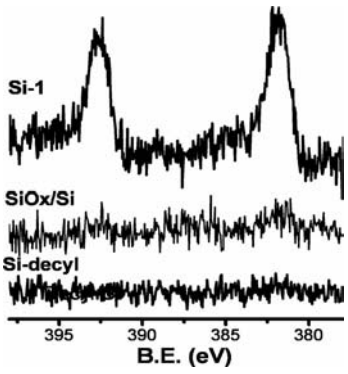

Figure 6. High resolution U 4f XPS spectra of various surfaces treated with uranyl solutions: **Si-1** (upper spectrum), **SiO_x/Si** (middle spectrum) and **Si-decyl** (bottom spectrum).

No significant signals are detected in the spectra of uranyl-treated **SiO_x/Si** and **decyl-Si**, proving that salen is required for uranyl coordination. The theoretical atomic ratio between U and N in the uranyl complex is 1/8, hence the complexation yield can be estimated from the measured U/N atomic ratio (ca. 1/15) as follows:

$$\text{Complexation yield (\%)} = \frac{\%U}{\%N} \times \frac{8}{1} \times 100$$

The thus obtained complexation yield was found to be in the 50–60% range.

Conclusions

New hybrid organic-inorganic materials consisting of quinoxaline cavitand-salen monolayers covalently bonded to flat and porous silicon have been synthesized. The success of the grafting protocol has been demonstrated by combining different analytic techniques (XPS, FTIR and AFM) with control experiments performed in the absence of UV or thermal activation. The results from this work indicate that molecules of **1** are covalently grafted to the silicon surface through a hydrosilylation reaction, but after anchoring further interactions occur between the salen nitrogen atoms s and the Si–OH termination groups of the oxidized surfaces through nitrogen protonation or H-bonding.

In addition, a surface-based synthetic route has been developed for the preparation of metal-salen complexes directly on a functionalized surface. This synthetic route is based on the reaction between the **Si-1** surface and uranyl acetate solution. The results from this experiment proved that the preparation of a system with different recognition properties was achieved, and it also showed that the salen reactivity, and hence its structural integrity, are kept after it is covalently anchored to the Si surface.

The functional flat and porous materials described in this work represent a useful addition to the available pool of hybrid systems that are suited for silicon integration. Moreover, these results show the potential of covalent grafting of organic molecules for the synthesis of a variety of functional materials based on specifically designed receptors.

Experimental Section

General: All reactions were carried out under nitrogen, and dry ethanol was used. All chemicals were reagent grade and were used without further purification.

The water used for porous silicon and monolayer preparations was of Milli-Q grade (18.2 MΩ cm) and was filtered through a 0.22 μm filter.

NMR experiments were carried out at 27 °C on a Varian UNITY Inova 500 MHz spectrometer (^{1}H NMR at 499.88 MHz, ^{13}C NMR at 125.7 MHz, samples in $CDCl_3$) equipped with pulse field-gradient module (*z* axis) and a tunable 5 mm Varian inverse detection probe (ID-PFG). Chemical shifts (ppm) were referenced to tetramethylsilane (TMS). EI-MS were obtained on an EI-MS Thermo-Finnigan LCQ-DECA spectrometer equipped with an ion trap analyzer. A JASCO V-560 UV/Vis spectrophotometer equipped with a 1 cm path-length cell was used for the UV/Vis titrations.

Synthesis of Aldehyde 3: To a stirred solution of 3-hydroxysalicylaldehyde (300 mg, 2.16 mmol) and K_2CO_3 (147 mg, 1.07 mmol) in dry acetonitrile (150 mL) a solution of 11-bromo-1-undecene (336 mg, 2.16 mmol) was added dropwise over a 4 h period at room temperature. The mixture was allowed to stir at room temperature for 2 d and then refluxed for 24 h. Solvent was removed under reduced pressure and the solid residue was purified by flash chromatography ($CHCl_3$/EtOAc, 95:5) to afford 144 mg (23% yield) of compound **3**. ^{1}H NMR (500 MHz, $CDCl_3$, 27 °C): δ = 11.08 (br. s, 1 H, O*H*), 9.88 (s, 1 H, C*H*O), 7.18 (d, *J* = 8.0 Hz, 1 H, Ar*H*), 7.14 (d, *J* = 8.0 Hz, 1 H, Ar*H*), 6.94 (t, *J* = 8.0 Hz, 1 H, Ar*H* in the *para*-position relative to OH), 5.81 (m, 1 H, C*H*=CH_2), 4.96 (dd, *J* = 17.0, 10.0 Hz, 2 H, CH=CH_2), 3.39 (t, *J* = 7.0 Hz, 2 H, O-CH_2-), 2.04 (q, *J* = 7.0 Hz, 2 H, -CH_2-CH=CH_2), 1.84 (m, 2 H, -CH_2-), 1.36–1.43 (m, 4 H, -CH_2-), 1.29 (m, 8 H, -CH_2-) ppm. ^{13}C NMR (125 MHz, $CDCl_3$, 27 °C): δ = 25.7, 28.8, 29.0, 29.30, 29.37, 30.0, 33.7, 77.4, 114.1, 120.9, 121.7, 124.7, 129.1, 139.0, 148.7, 149.6, 189.7 ppm. EI-MS: *m*/*z* = 291 $[M + H]^+$. $C_{18}H_{26}O_3$ (290.00): calcd. C 74.45, H 9.02; found C 74.42, H 9.04.

Synthesis of the Mono-imino-amine Derivative 4: (1*R*,2*R*)-Diphenylethylenediamine chloride (0.52 g, 2.1 mmol) was dissolved in a 1:1 mixture of ethanol/methanol (20 mL). To this diamine solution, a solution of **3** (0.49 g, 2.1 mmol) in a 1:1 mixture of ethanol/methanol (20 mL) was added dropwise. The mixture was stirred for 24 h, and then the solvent was removed under reduced pressure. The solid residue was washed with water and diethyl ether to give 0.88 g of **4** (90% yield). ^{1}H NMR (500 MHz, $CDCl_3$, 27 °C): δ = 8.17 (s, 1 H, C*H*N), 7.17–7.25 (m, 10 H, Ar*H*), 6.69 (m, 2 H, Ar*H*), 5.81 (m, 1 H, C*H*=CH_2), 4.96 (dd, *J* = 17.0, 10.0 Hz, 2 H, CH=CH_2), 4.79 (s, 2 H, C*H* methine), 3.40 (t, *J* = 7.0 Hz, 2 H, O-CH_2-), 2.04 (q, *J* = 7.0 Hz, 2 H, -CH_2-CH=CH_2), 1.86 (m, 2 H,-CH_2-), 1.36–1.44 (m, 4 H, -CH_2-), 1.30 (m, 8 H, -CH_2-) ppm. ^{13}C NMR (125 MHz, $CDCl_3$, 27 °C): δ = 166.3, 149.9, 145.1, 139.2, 139.0, 128.6, 127.9, 127.6, 122.5, 118.6, 117.7, 117.5, 114.1, 79.1, 33.9, 33.7, 32.8, 29.3, 29.0, 28.9, 28.7, 28.1 ppm. EI-MS: *m*/*z* = 485 $[M]^+$. $C_{32}H_{41}ClN_2O_2$ (520.47): calcd. C 73.75, H 7.93, N 5.38; found C 73.71, H 7.89, N 5.35.

Synthesis of 1: In a round-bottomed flask monoformyl cavitand **2**[14] (360 mg, 0.293 mmol) and mono-imino-amine chloride **4** (150 mg, 0.293 mmol) were dissolved in absolute ethanol (100 mL). An excess of triethylamine (150 μL) was added to this mixture and the reaction was stirred at room temperature overnight. The reaction was monitored by TLC (hexane/EtOAc, 70:30), and the solvent was removed after TLC indicated that all the starting cavitand had disappeared from the reaction solution. The solid residue was purified by flash chromatography (hexane/EtOAc, 70:30) to afford 80 mg of receptor **1** (17% yield). ^{1}H NMR (500 MHz, $CDCl_3$, 27 °C): δ = 15.55 (br. s, 1 H, O*H*), 10.77 (s, 1 H, O*H*), 10.74 (s, 1 H, O*H*), 8.43 (s, 1 H, C*H*N), 8.34 (s, 1 H, C*H*N), 8.01 (dd, *J* = 8.0, 1.5 Hz, 1 H, Ar*H*), 7.98 (d, *J* = 5 Hz, 1 H, Ar*H*), 7.95 (s, 1 H, Ar*H*), 7.79–7.84 (m, 2 H, Ar*H*), 7.73 (dd, *J* = 8.0, 1.0 Hz, 1 H, Ar*H*), 7.71 (s, 1 H, Ar*H*), 7.51–7.64 (m, 11 H, Ar*H*), 7.50 (s, 1 H, Ar*H*), 7.44 (m, 2 H, Ar*H*), 7.35 (s, 1 H, Ar*H*), 7.23 (s, 1 H, Ar*H*), 7.18 (d, *J* = 1.5 Hz, 1 H, Ar*H*), 7.10–7.13 (m, 2 H, Ar*H*), 7.06 (d, *J* = 8.5 Hz, 1 H, Ar*H*), 7.02–7.04 (m, 1 H, Ar*H*), 6.92 (dd, *J* = 8.0, 2.5 Hz, 1 H, Ar*H*), 6.79 (dd, *J* = 8.0, 2.5 Hz, 1 H, Ar*H*), 6.66 (d, *J* = 7.0 Hz, 1 H, Ar*H*), 5.69 (t, *J* = 8.0 Hz, 1 H, C*H* methine), 5.65 (t, *J* = 8.0 Hz, 1 H, C*H* methine), 5.57 (m, 2 H, C*H*=CH_2), 4.97 (dd, *J* = 17.0, 10.0 Hz, 2 H, CH=CH_2), 4.81 (t, *J* = 8.0 Hz, 1 H, C*H* methine), 4.51 (d, *J* = 7.0 Hz, 1 H, C*H* methine), 4.55–4.70 (m, 10 H, -CH_2-), 3.94 (t, *J* = 8.0 Hz, 1 H, C*H* methine), 2.28–2.41 (m, 18 H, -CH_2-), 2.20 (m, 2 H, -CH_2-), 2.12 (m, 2 H, -CH_2-), 1.30–1.50 (m, 24 H, -CH_2-), 0.90 (t, *J* = 7.5 Hz, 9 H, -CH_3), 0.71 (t, *J* = 7.5 Hz, 3 H, -CH_3) ppm. EI-MS: *m*/*z* = 1743 $[MH + C_2H_5OH]^+$. $C_{109}H_{116}N_8O_{10}$ (1698.16): calcd. C 77.09, H 6.89, N 6.60; found C 77.13, H 6.87, N 6.57.

Porous Silicon Preparation: Porous silicon (**PSi**) has been obtained by wet metal-assisted chemical etching according to the procedure reported by Chartier et al.[31] Briefly, Si(100) slides were dipped for 5 min in an aqueous solution of HF (0.14 M) and $AgNO_3$ (5×10^{-4} M) to deposit Ag particles on the surface. The slides were then etched in aqueous solutions containing HF, H_2O_2 and ultra-

pure H_2O (40% HF, 30% H_2O_2 and H_2O in a 25:10:4 ratio) for 1 min, and after etching the samples were rinsed with ultra-pure water and dried with prepurified N_2.

The thickness and morphology of the etched layer were checked by SEM cross-section analysis (Figure S2a), and are consistent with those reported in literature for Ag-assisted chemical etching.

Monolayer Preparation: Compound **1** (34 mg) was dissolved in mesitylene (4.0 mL, 0.005 M). The solution was placed in a quartz cell and deoxygenated by stirring in a dry box for at least 1 h. To graft **1** on flat silicon, Si(100) slides were first cleaned in "piranha" solution (concd. H_2SO_4 and 35% H_2O_2, 70:30 v/v) at room temperature for 12 min, rinsed in ultra-pure water for 2 min, etched in 1.0% hydrofluoric acid for 90 s, washed with ultra-pure water for 10 s, dried with N_2, and then immediately placed in the solution of **1**. The cell remained under UV irradiation (254 nm) for 2 h in the dry box.

To graft **1** onto porous substrates, **PSi** was etched in 10% HF solution for 1 h, washed with ultra-pure water for 20 s, dried with N_2, and immediately placed in the solution of **1**. The solution was then refluxed at 200 °C for 5 h, with a slow stream of N_2 bubbling through the solution to prevent bumping.

After grafting, both the flat and porous samples were removed from the solution of **1** (after cooling to room temperature in the case of **PSi**) and cleaned by two rinsing cycles of ultrasonic cleaner (5 min each) in dichloromethane.

The SEM cross-section analysis of **PSi-1** (Figure S2b) showed that the sample had a morphology similar to that observed for the **PSi** substrate before grafting (Figure S2a), indicating that the anchoring method did not significantly degrade the structure of porous silicon.

Surface Reaction Experiments: Uranyl-salen complexes were obtained directly on the silicon surface by reacting **Si-1** with uranyl acetate solutions. To validate the results obtained with the **Si-1** surface, the same reaction process was repeated with inert surfaces, namely native silicon oxide (**SiO_x/Si**) and decyl-functionalized silicon (**Si-decyl**). The **Si-decyl** substrate was prepared as follows: 1-decene (10 mL) was placed in a quartz cell, deoxygenated by stirring in a dry box for at least 1 h and then grafted with the decyl group according to the same procedure described above for **Si-1** preparation. Surface reaction experiments were performed by dipping **Si-1**, **SiO_x/Si** and **Si-decyl** surfaces into a solution of uranyl acetate (10^{-3} M) in ethanol for 1 h at 20 °C. Samples were then repeatedly rinsed with EtOH and water, and then dried under a nitrogen gas stream.

Surface Characterization: XPS spectra were run with a PHI 5600 multi-technique ESCA-Auger spectrometer equipped with a monochromated Al K_α X-ray source. Analyses were carried out with a photoelectron angle of 45° (relative to the sample surface) with an acceptance angle of ± 7°. The XPS binding energy (BE) scale was calibrated by centring the C 1s peak due to hydrocarbon moieties and "adventitious" carbon at 285.0 eV.[32] Transmission FTIR measurements were recorded on a JASCO FTIR 430, with 100 scans collected per spectrum (scan range 560–4000 cm^{-1}, resolution 4 cm^{-1}). AFM images were obtained in high amplitude mode (tapping mode) by a NT-MTD Solver P47 instrument. The noise level before and after each measurement was 0.01 nm. SEM micrographs were obtained with a LEO SUPRA 55VP equipped with a field emission gun.

Supporting Information (see footnote on the first page of this article): Details of the solution complexation tests involving the trimethylammonium ion. Figure S1: UV/Vis titration between receptor **1** and *N*,*N*,*N*-trimethyl-α-methyl-benzylammonium iodide. Figure S2: SEM cross-section of **PSi** before and after grafting of receptor **1** onto the surface.

Acknowledgments

This work was finacially supported by Consorzio Interuniversitario Nazionale per la Scienza e la Tecnologia dei Materiali (INSTM) through PRISMA "Molecular systems grafted on silicon for integrated sensing devices" project and by Ministero dell' Istruzione, dell' Università e della Ricerca (MIUR) through the FIRB "ITALNANONET" RBPR05JH2P project. We acknowledge the CINECA award N. HP10B0RIE4 for the availability of high performance computing resource and support. Also we thank University of Catania for financial support.

[1] a) G. Ashkenas, D. Cahen, R. Cohen, A. Shanzer, A. Vilan, *Acc. Chem. Res.* **2002**, *35*, 121–128; b) G. P. Lopinski, D. D. M. Wayner, R. A. Wolkow, *Nature* **2000**, *406*, 48–51; c) A. Ulman, *Chem. Rev.* **1996**, *96*, 1533–1554.

[2] a) T. P. Sullivan, W. T. S. Huck, *Eur. J. Org. Chem.* **2003**, 17–29; b) A. Ulman, *Adv. Mater.* **2004**, *16*, 573–582; c) S. Onclin, B. J. Ravoo, D. N. Reinhoudt, *Angew. Chem. Int. Ed.* **2005**, *44*, 6282–6304; d) G. Lopinski, *Int. J. Nanotechnol.* **2008**, *5*, 1247–1267.

[3] a) Z. Liu, A. A. Yassery, J. S. Lindsey, D. F. Bocian, *Science* **2003**, *302*, 1543–1545; b) A. Gulino, F. Lupo, G. G. Condorelli, M. E. Fragalà, M. E. Amato, G. Scarlata, *J. Mater. Chem.* **2008**, *18*, 5011–5018; c) A. Gulino, F. Lupo, G. G. Condorelli, A. Motta, I. L. Fragalà, *J. Mater. Chem.* **2009**, *19*, 3507–3511.

[4] D. D. Gandhi, M. Lane, Y. Zhou, A. P. Singh, S. Nayak, U. Tisch, M. Eizenberg, G. Ramanath, *Nature* **2007**, *447*, 299–302.

[5] a) M. Halik, H. Klauk, U. Zschieschang, G. Schmid, C. Dehm, M. Schütz, S. Maisch, F. Effenberger, M. Brunnbauer, F. Stellacci, *Nature* **2004**, *431*, 963–966; b) T. Gupta, M. E. van der Boom, *Angew. Chem. Int. Ed.* **2008**, *47*, 5322–5326.

[6] a) G. G. Condorelli, A. Motta, I. L. Fragalà, F. Giannazzo, V. Raineri, A. Caneschi, D. Gatteschi, *Angew. Chem. Int. Ed.* **2004**, *43*, 4081–4084; b) M. Mannini, F. Pineider, P. Sainctavit, C. Danieli, E. Otero, C. Sciancalepore, A. M. Talarico, M.-A. Arrio, A. Cornia, D. Gatteschi, R. Sessoli, *Nat. Mater.* **2009**, *8*, 194–197.

[7] a) C. Bartic, A. Campitelli, G. Borghi, *Appl. Phys. Lett.* **2003**, *82*, 475–477; b) F. Mancin, E. Rampazzo, P. Tecilla, U. Tonellato, *Chem. Eur. J.* **2006**, *12*, 1844–1854; c) A. Gulino, S. Bazzano, G. G. Condorelli, S. Giuffrida, P. Mineo, C. Satriano, E. Scamporrino, G. Ventimiglia, D. Vitalini, I. L. Fragalà, *Chem. Mater.* **2005**, *17*, 1079–1084.

[8] a) J. Rebek, *Angew. Chem. Int. Ed. Engl.* **1990**, *29*, 245–255; b) C. H. Hunter, K. R. Lawson, J. Perkins, C. J. Urch, *J. Chem. Soc. Perkin Trans. 2* **2001**, 651–669; c) R. Pinalli, M. Suman, E. Dalcanale, *Eur. J. Org. Chem.* **2004**, 451–462; d) M. Suman, N. Bouzouane, E. Barbieri, F. Ugozzoli, E. Dalcanale, *J. Supramol. Chem.* **2002**, *2*, 97–106; e) L. Pirondini, E. Dalcanale, *Chem. Soc. Rev.* **2007**, *36*, 695–706; f) A. Gulino, T. Gupta, M. Altman, S. Lo Schiavo, P. G. Mineo, I. L. Fragalà, G. Evmenenco, P. Dutta, M. E. van der Boom, *Chem. Commun.* **2008**, 2900–2902.

[9] G. G Condorelli, A. Motta, M. Favazza, I. L. Fragalà, M. Busi, E. Menozzi, E. Dalcanale, L. Cristofolini, *Langmuir* **2006**, *22*, 11126–11133.

[10] E. Biavardi, M. Favazza, A. Motta, I. L. Fragalà, C. Massera, L. Prodi, M. Montalti, M. Melegari, G. G. Condorelli, E. Dalcanale, *J. Am. Chem. Soc.* **2009**, *131*, 7447–7455.

[11] G. G. Condorelli, A. Motta, M. Favazza, E. Gurrieri, P. Betti, E. Dalcanale, *Chem. Commun.* **2010**, *46*, 288–290.

[12] a) A. G. Cullis, L. T. Canham, *Nature* **1991**, *353*, 335–338; b) J. M. Buriak, *Chem. Rev.* **2002**, *102*, 1271–1308; c) J. M. Buriak, *Phil. Trans. R. Soc. A* **2006**, *364*, 217–225.
[13] a) M. E. Amato, F. P. Ballistreri, A. Pappalardo, G. A. Tomaselli, R. M. Toscano, D. J. Williams, *Eur. J. Org. Chem.* **2005**, 3562–3570; b) M. E. Amato, F. P. Ballistreri, A. Pappalardo, D. Sciotto, G. A. Tomaselli, R. M. Toscano, *Tetrahedron* **2007**, *63*, 9751–9757; c) A. Patti, S. Pedotti, F. P. Ballistreri, G. Trusso Sfrazzetto, *Molecules* **2009**, *14*, 4312–4325; d) M. E. Amato, F. P. Ballistreri, S. Gentile, A. Pappalardo, G. A. Tomaselli, R. M. Toscano, *J. Org. Chem.* **2010**, *75*, 1437–1443; e) F. P. Ballistreri, A. Pappalardo, G. A. Tomaselli, R. M. Toscano, G. Trusso Sfrazzetto, *Eur. J. Org. Chem.* **2010**, 3806–3810.
[14] F. P. Ballistreri, A. Pappalardo, G. A. Tomaselli, G. Trusso Sfrazzetto, E. Vittorino, S. Sortino, *New J. Chem.* **2010**, *34*, 2828–2834.
[15] a) S. Richeter, J. Rebek Jr., *J. Am. Chem. Soc.* **2004**, *126*, 16280–16281; b) A. Gissot, J. Rebek Jr., *J. Am. Chem. Soc.* **2004**, *126*, 7424–7425; c) E. Menozzi, H. Onagi, A. L. Rheingold, J. Rebek Jr., *Eur. J. Org. Chem.* **2005**, 3633–3636; d) M. Cametti, M. Nissinen, A. Dalla Cort, L. Mandolini, K. Rissanen, *J. Am. Chem. Soc.* **2007**, *129*, 3641–3648.
[16] a) A. Bansal, X. Li, S. I. Yi, W. H. Weinberg, N. S. Lewis, *J. Phys. Chem. B* **2001**, *105*, 10266–10277; b) G. F. Cerofolini, C. Galati, S. Lorenti, L. Renna, O. Viscuso, C. Bongiorno, V. Raineri, C. Spinella, G. G. Condorelli, I. L. Fragalà, A. Terrasi, *Appl. Phys. A* **2003**, *77*, 403–409.
[17] a) A. S. Killampalli, P. F. Ma, J. R. Engstrom, *J. Am. Chem. Soc.* **2005**, *127*, 6300–6310; b) A. Gulino, F. Lupo, G. G. Condorelli, P. Mineo, I. L. Fragalà, *Chem. Mater.* **2007**, *19*, 5102–5109; c) A. Dube, A. R. Chadeayne, M. Sharma, P. T. Wolczanski, J. R. Engstrom, *J. Am. Chem. Soc.* **2005**, *127*, 14299–14309.
[18] a) D. Briggs, in: *Practical Surfaces Analysis* (Eds.: D. Briggs, M. P. Seah), Wiley-VCH, Weinheim, Germany, **1995**, 2nd ed., vol. 1, p. 444; b) G. Beamson, D. Briggs, *High-Resolution XPS of Organic Polymers*, The Scienta ESCA300 Database, Wiley & Sons, New York, **1992**.
[19] a) G. F. Cerofolini, C. Galati, S. Reina, L. Renna, O. Viscuso, G. G. Condorelli, I. L. Fragalà, *Mater. Sci. Eng. C* **2003**, *23*, 989–994; b) G. F. Cerofolini, C. Galati, S. Reina, L. Renna, *Mater. Sci. Eng. C* **2003**, *23*, 253–257.
[20] a) A. Vesel, M. Mozetic, A. Zalar, *Vacuum* **2008**, *82*, 248–251; b) A. P. Pijpers, R. J. Meier, *Chem. Soc. Rev.* **1999**, *28*, 233–238.
[21] a) J. M. Gottfried, K. Flechtner, A. Kretschmann, T. Lukasczyk, H. P. Steinruck, *J. Am. Chem. Soc.* **2006**, *128*, 5644–5645; b) M. Lu, B. Chen, T. He, Y. Li, J. M. Tour, *Chem. Mater.* **2007**, *19*, 4447–4453.
[22] a) S. J. Kerber, J. J. Bruckner, K. Wozniak, S. Seal, S. Hardcastle, T. L. Barr, *J. Vac. Sci. Technol. A* **1996**, *14*, 1314–1320; b) J. N. O'Shea, J. Schnadt, P. A. Brühwiler, H. Hillesheimer, L. Patthey, J. Krempasky, C. Wang, Y. Luo, H. Agren, *J. Phys. Chem. B* **2001**, *105*, 1917–1920.
[23] a) S. W. Ong, X. L. Zhao, K. B. Eisenthal, *Chem. Phys. Lett.* **1992**, *191*, 327–335; b) Y. Duval, J. A. Mielczarski, O. S. Pokrovsky, E. Mielczarski, J. J. Ehrhardt, *J. Phys. Chem. B* **2002**, *106*, 2937–2945; c) K. Leung, I. M. B. Nielsen, L. J. Criscenti, *J. Am. Chem. Soc.* **2009**, *131*, 18358–18365.
[24] a) H. C. Choi, J. M. Buriak, *Chem. Mater.* **2000**, *12*, 2151–2156; b) G. Mattei, V. Valentini, V. A. Yakovlev, *Surf. Sci.* **2002**, *502–503*, 58–62; c) S. A. Alekseev, V. Lysenko, V. N. Zaitsev, D. Barbier, *J. Phys. Chem. C* **2007**, *111*, 15217–15222.
[25] a) F. Ozanam, J. N. Chazalviel, *J. Electroanal. Chem.* **1989**, *269*, 251; b) D. B. Mawhinney, J. A. Glass, J. T. Yates, *J. Phys. Chem. B* **1997**, *101*, 1202–1206; c) W. Haiss, P. Raisch, D. J. Schiffrin, L. Bitsch, R. J. Nichols, *J. Chem. Soc. Faraday Trans.* **2002**, *121*, 167–180.
[26] a) R. Hofman, J. G. F. Westheim, I. Pouwel, T. Fransen, P. J. Gellings, *Surf. Inter. Anal.* **1996**, *24*, 1–6; b) F. Massines, N. Gherardi, A. Fornelli, S. Martin, *Surf. Coat. Technol.* **2005**, *200*, 1855–1861; c) B. B. Burton, S. W. Kang, S. W. Rhee, S. M. Gorge, *J. Phys. Chem. C* **2009**, *113*, 8249–8257.
[27] X. N. Xie, H. J. Chung, C. H. Sow, A. T. S. Wee, *Mater. Sci. Eng. R* **2006**, *54*, 1–48.
[28] a) G. G. Condorelli, C. Tudisco, A. Motta, A. Di Mauro, F. Lupo, A. Gulino, I. L. Fragalà, *Eur. J. Inorg. Chem.* **2010**, 4121–4129; b) A. Motta, G. G. Condorelli, A. Pellegrino, A. Cornia, I. L. Fragalà, *J. Phys. Chem. C* **2010**, *114*, 20696–20701.
[29] D. M. Singer, F. Farges, G. E. Brown Jr., *Geochim. Cosmochim. Acta* **2009**, *73*, 3593–3611.
[30] D. Chadwick, *Chem. Phys. Lett.* **1973**, *21*, 291–294.
[31] C. Chartier, S. Bastide, C. Lèvy-Clèment, *Electrochim. Acta* **2008**, *53*, 5509–5516.
[32] a) I. L. Swift, *Surf. Interface Anal.* **1982**, *4*, 47–51; b) D. Briggs, G. Beamson, *Anal. Chem.* **1992**, *64*, 1729–1736.

Received: November 25, 2010
Published Online: March 15, 2011

